Supporting Information

Triple-enhanced Raman Scattering Sensors from Flexible MXene/Au Nanocubes Platform via Attenuating the Coffee Ring Effect

Xin Liu[1,2], *Alei Dang*[1,2]*, *Tiehu Li*[1,2]*, *Tung-Chun Lee*[3,4], *Yiting Sun*[1,2], *Yuhui Liu*[1,2], *Fei Ye*[1,2], *Shuze Ma*[1], *Yong Yang*[1], *Weibin Deng*[1,2]

[1.] School of Materials Science and Engineering, Northwestern Polytechnical University, Xi'an 710072, P. R China.

[2.] Shannxi Engineering laboratory for Graphene New Carbon Materials and Applications, School of Materials Science and Engineering, Northwestern Polytechnical University, Xi'an 710072, P. R China.

[3.] Department of Chemistry, University College London (UCL), London WC1H 0AJ, U.K.

[4.] Institute for Materials Discovery, University College London, London, WC1H 0AJ, UK.

*Corresponding author: Alei Dang, Tiehu Li

E-mail address: dangalei@nwpu.edu.cn; litiehu@nwpu.edu.cn;

Table of Contents

1. Calculation of Raman Enhanced Factor (EF)

The following equation is used to calculate the enhancement factor:

$$EF = \frac{(I_{SERS}/N_{SERS})}{(I_{REF}/N_{REF})} \quad \text{(S1)}$$

where N_{SERS} and N_{REF} are the number of probe molecules in the excitation volume of the MXene/AuNCs-FOTS composite membranes and reference, respectively, and I_{SERS} and I_{REF} are the Raman signal intensities at 612 cm^{-1} obtained from MXene/AuNCs-FOTS composite membranes and 10^{-3} M R6G solution under 532 nm laser irradiation.

Calculation of N_{SERS}:

According to the experiment, approximately 5 μl (V_1) of 10^{-10} M (C_1) R6G solution was absorbed on the surface of the 5.2 mm^2 membranes (S_1). Raman's laser spot diameter is approximately 5 μm (d). Therefore, the number of excited probe molecules can be calculated in the following way:

$$N_{SERS} = \left(\frac{\pi d^2}{4 \times S_1}\right) \times V_1 \times C_1 \times N_A \quad \text{(S2)}$$

Calculation of N_{REF}:

The laser can easily pass through the R6G solution (C_2=10^{-3} M), and the illuminated volume (V_2) is approximately 6.25×10^{-14} m^3. Then, the number of probe molecules being illuminated in the reference Raman measurement can be calculated as:

$$N_{REF} = V_2 \times C_2 \times N_A \quad \text{(S3)}$$

From this, the EF can be calculated.

2. Calculation of contact angle and contact area

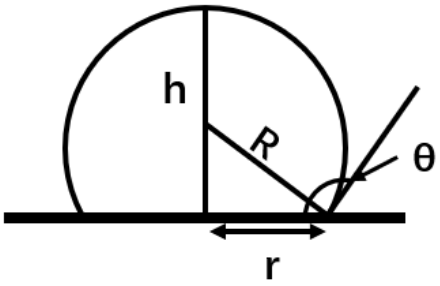

First, assume that the volume of the droplet is V, the radius of the droplet is R, the height is h, the contact angle with the membranes is θ, and the contact area is $r^2\pi$. Therefore, the following relationship exists:

$$r = Rsin\,\theta \tag{S4}$$

$$h = (1 - \cos\theta)R \tag{S5}$$

$$V = \frac{\pi}{3}h^2(3R - h) \tag{S6}$$

Further:

$$R = \frac{r}{\sin\theta} \tag{S7}$$

$$h = r\,tan\,\frac{\theta}{2} \tag{S8}$$

Therefore, the relationship between the contact angle and the contact area is described as:

$$V = \frac{\pi}{3}r^3\,tan^2\frac{\theta}{2}\left(\frac{3}{\sin\theta} - \tan\frac{\theta}{2}\right) \tag{S9}$$

Since the droplet volume V is 5 μl, the change law of the contact area can be easily obtained when the contact angle changes.

3. Estimation of AuNCs concentration by UV-vis spectra

The concentrations of AuNCs were roughly estimated from UV-vis spectra by the previously reported method[1]:

$$C = \frac{A_{450}\times 10^{14}}{d^2[-0.295+1.36\exp\,(-(\frac{d-96.8}{78.2})^2)]}\times\frac{1}{N_A} \tag{S10}$$

Where C is the molar concentration, A_{450} is the absorbance at λ = 450 nm, d is the side length of AuNCs and N_A is Avogadro's constant.

4. Determination of the complex refractive index of Ti_3C_2 MXene

First, define the complex refractive index (n) of MXene as:

$$n = k + \alpha(\lambda/_k)i \quad \text{(S11)}$$

Where k is the real part of the refractive index, λ is the wavelength of the incident light, and α is the absorption coefficient. Previous calculations reported in detail the optical parameters of MXene [2, 3]. Therefore, in this work, λ =532 nm, $\alpha = 5.97\ \mu m^{-1}$ and $k = 2.39$. Substitution gives the complex refractive index (n) of Ti3C2 MXene as $= 2.39 + 1.33$i.

5. Synthesis of Au Nanocubes

Au nanocubes (AuNCs) with an average particle size of 66.8±5.4 nm were synthesized in large quantities by modifying a previously reported method[4]. Briefly, 0.25 ml of 0.01 M $HAuCl_4$ was added to 9.75 ml aqueous solution with 0.32 g CTAC under stirring, followed by the quick injection of 0.45 ml of 0.02 M ice-cold $NaBH_4$ solution and aged for 1 h at 30°C to form Au seeds solution. To prepare the growth solution, 96.25 ml of 0.1 M CTAC solution in a flask was brought to a temperature of 30°C before adding 2.5 ml of 0.01 M $HAuCl_4$, 0.1 ml of 0.01 M NaBr and 0.9 ml of 0.04 M AA sequentially. Next, 10 ml of growth solution was taken from the flask into the vial, and 25 μl of the previously prepared Au seed solution was added to the vial with shaking until the solution color turned light pink (~5 s). Then, 225 μl of the solution in vial was transferred to the flask with even mixing. Finally, the solution in the flask was left undisturbed for 30 min and centrifuged at 5000 rpm for 10 min to obtain the AuNCs. The produced AuNCs was adjusted by DI water to 15 nM for further using.

6. Synthesis of Ti_3C_2Tx MXene Nanosheets

$Ti_3C_2T_x$ MXene nanosheets were fabricated by an etching method. In a typical process, Ti_3AlC_2 powder (1 g) was slowly added to a premixed solution of LiF (1.6 g) and 20 ml (9 M) HCl and stirred for 24 h at 35°C. Next, the resulting solution was washed with concentrated HCl three times to remove excess lithium compounds and was further washed with DI water several times by centrifugation until pH>6. Finally, an ultrasonic cell pulverizer (Ningbo Xinzhi, JY88-IIN, 500 W) was used for sonication for 30 min, and the resulting product was centrifuged at 3500 rpm for 15 min. The supernatant was carefully collected, and mediated to 3 mg/ml for further membrane fabrication.

7. Theoretical Calculation

Commercial software (COMSOL) combined with the finite element method (FEM) was used to simulate electromagnetic coupling between AuNCs and Ti3C2Tx MXene. In the simulation, the side length and spacing of the AuNCs were modeled based on their TEM images. The incident wavelength is defined as 532 nm, and the dielectric constant values of gold are provided by the software. Ti3C2Tx MXene was defined as a 2 nm homogeneous layer, and the refractive index was set as n= 2.39 + 1.33i (see details in Supporting Information), and ultrafine grids were used to all materials to improve the calculation accuracy.

8. Supporting Figures

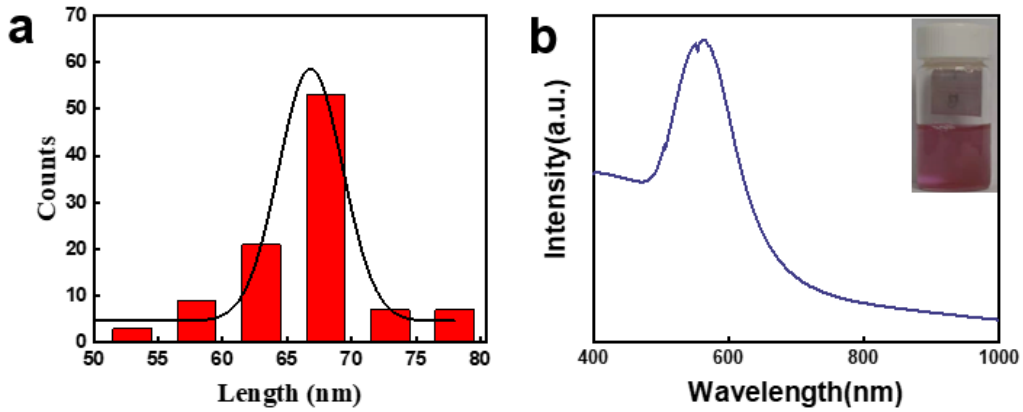

Figure S1. (a) Particle size distribution (66.8±5.4nm) and (b) the UV–vis spectra of AuNCs.

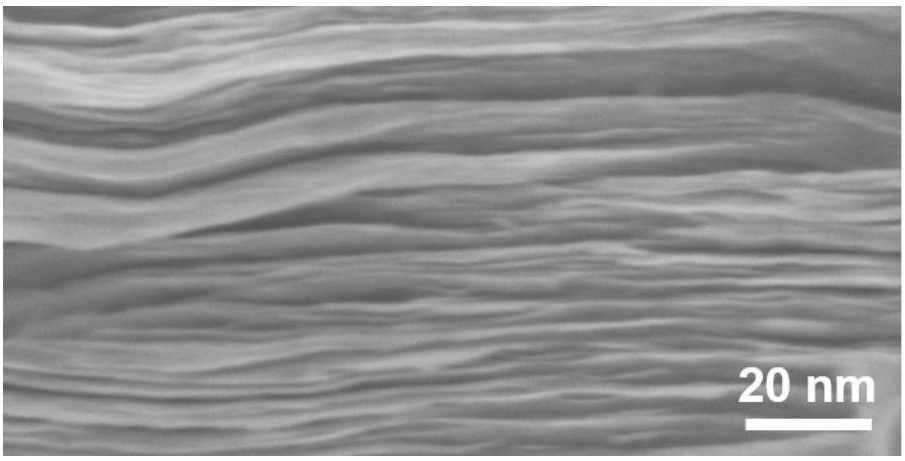

Figure S2. SEM image of the cross section of a $Ti_3C_2T_x$ MXene membrane.

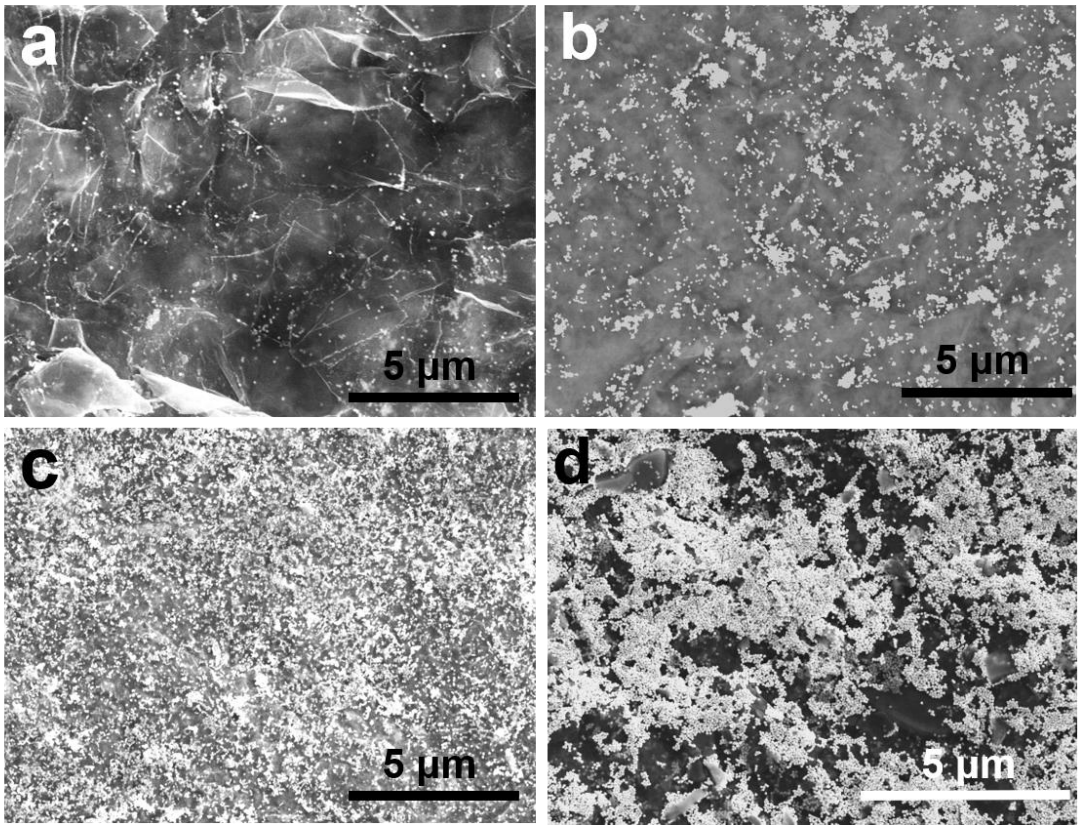

Figure S3. SEM images of composite membranes prepared with different concentrations of AuNCs.

(a) 3 nM, (b) 9 nM, (c) 15 nM and (d) 30 nM.

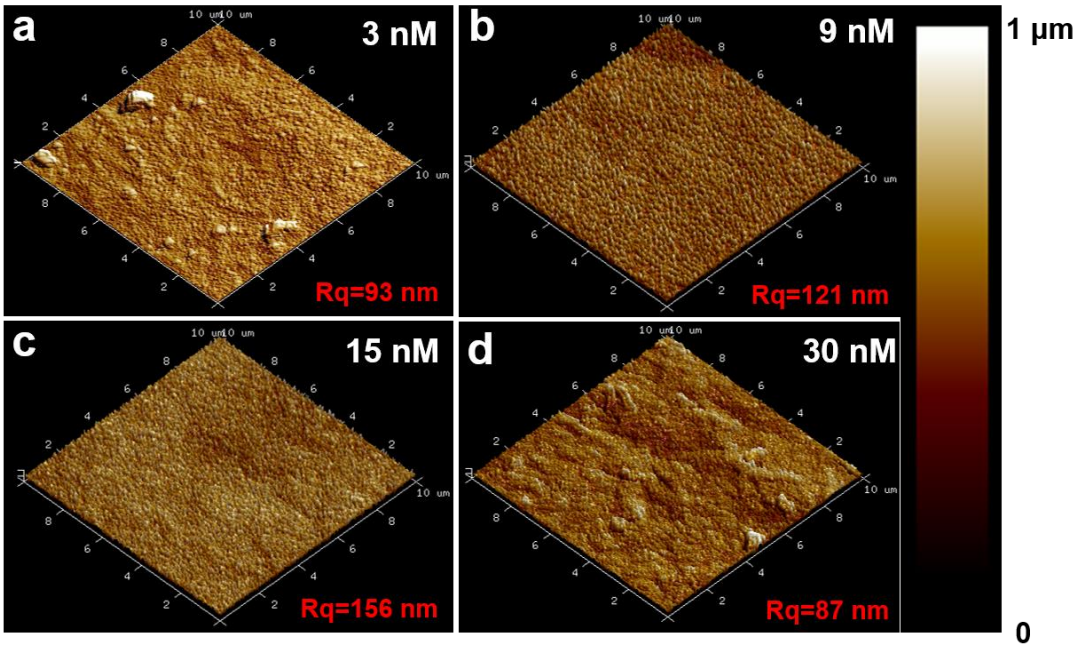

Figure S4. 3D AFM images mapped by height difference in 10×10 μm^2 to reflect the roughness of MXene/AuNCs membranes prepared with (a) 3 nM, (b) 9 nM, (c) 15 nM and (d) 30 nM concentrations of AuNCs**.**

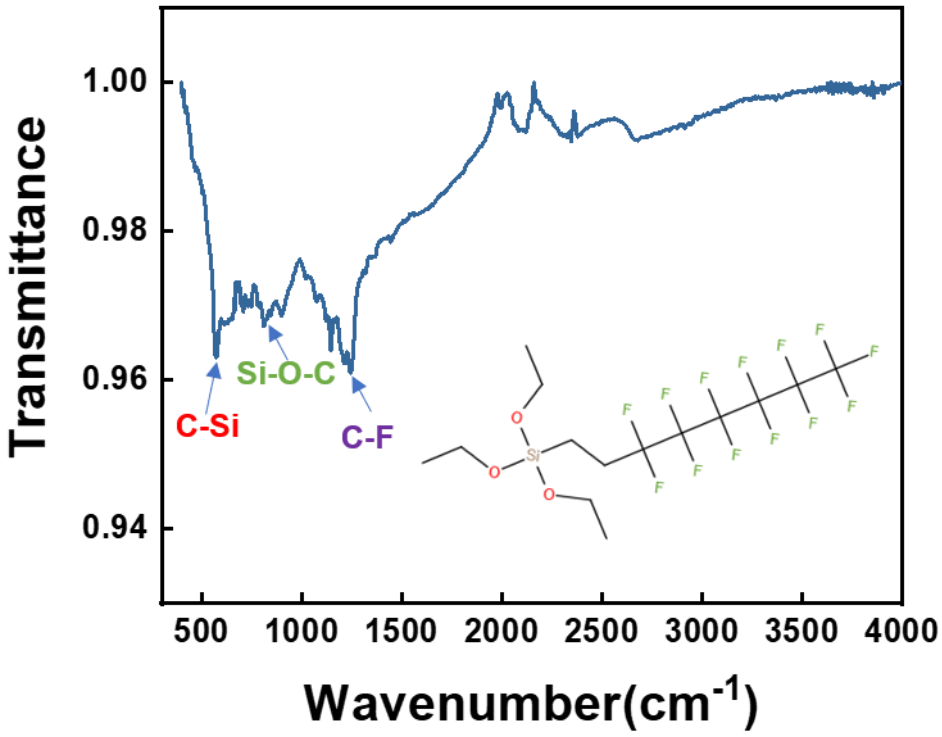

Figure S5. Infrared spectrum of MXene/AuNCs-FOTS membrane substrates.

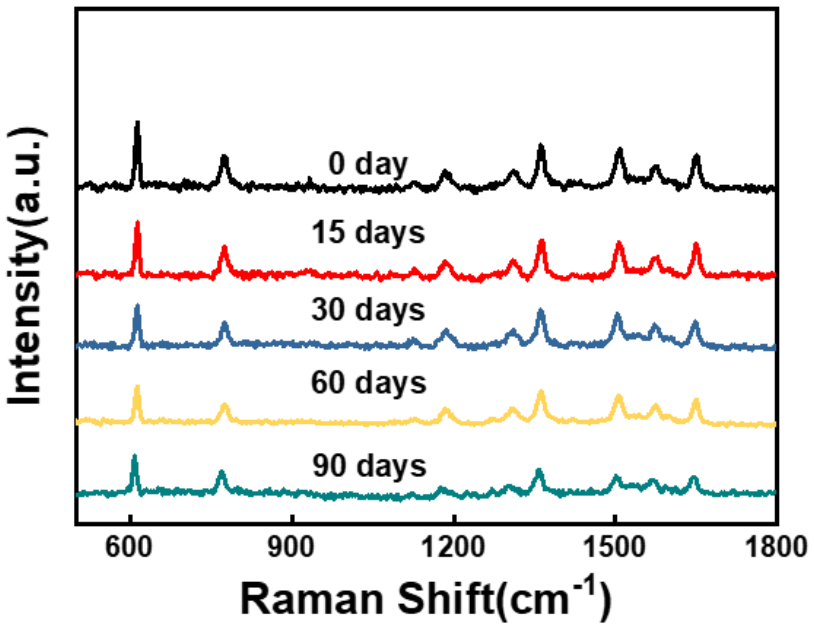

Figure S6. The SERS spectra of R6G collected from MXene/AuNCs membranes after storage in air for various times.

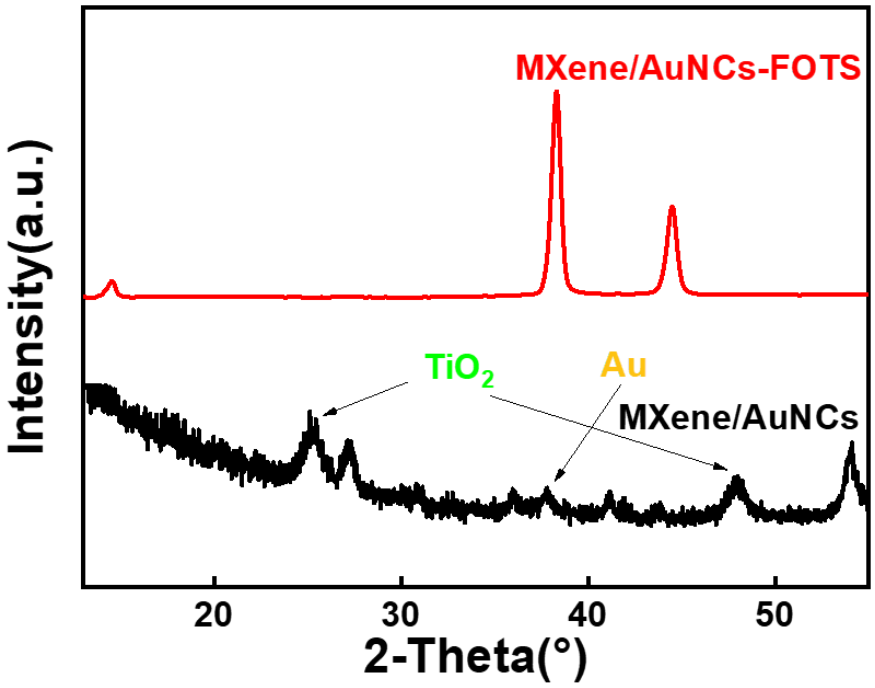

Figure S7. XRD of MXene/AuNCs-FOTS and MXene/AuNCs membranes stored in a humidified atmosphere (relative humidity ≈ 45 %) for 90 days.

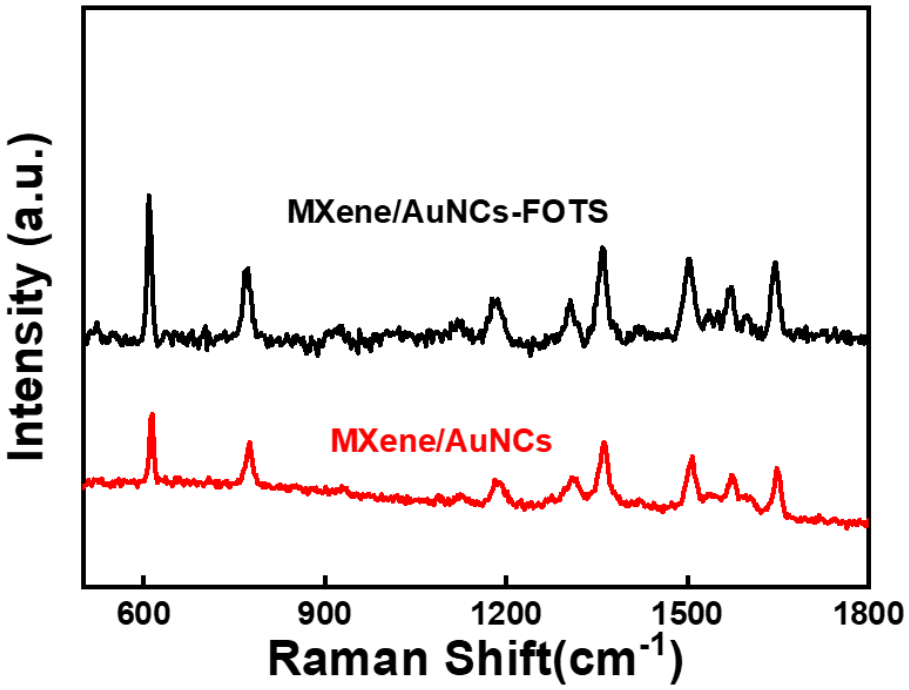

Figure S8. SERS spectra of 1×10^{-10} M R6G collected from MXene/AuNCs and MXene/AuNCs-FOTS membrane substrates.

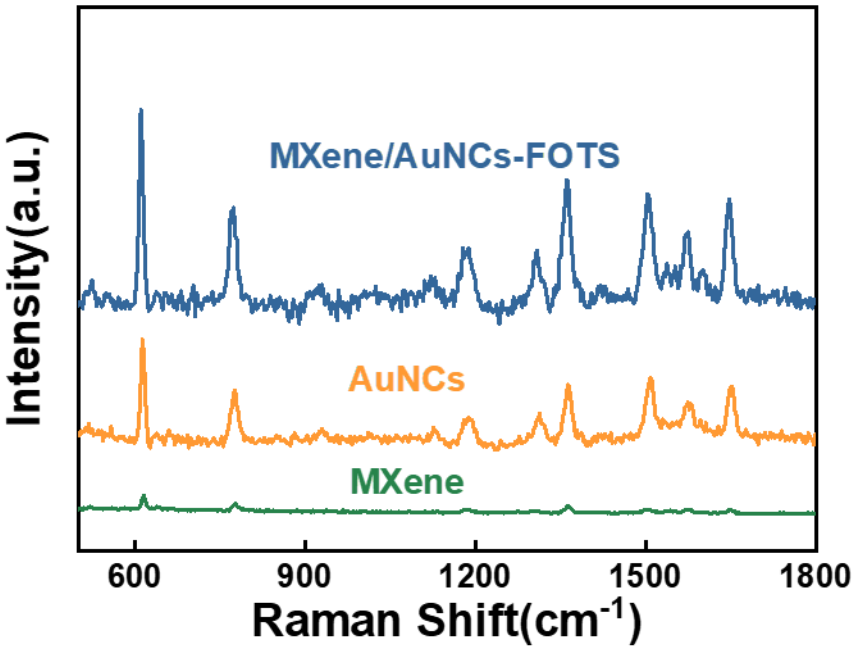

Figure S9. SERS spectra of 1×10^{-10} M R6G collected from $Ti_3C_2T_x$ MXene nansheets, AuNCs, and MXene/AuNCs-FOTS membrane substrates.

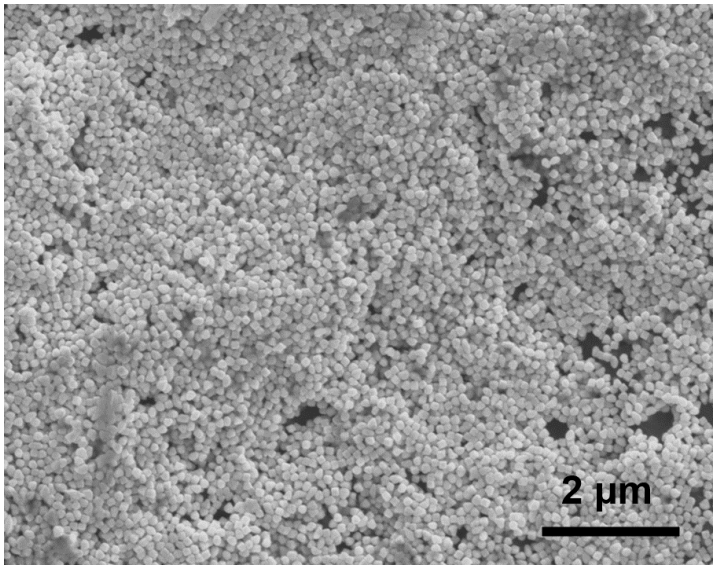

Figure S10. SEM image of AuNCs film.

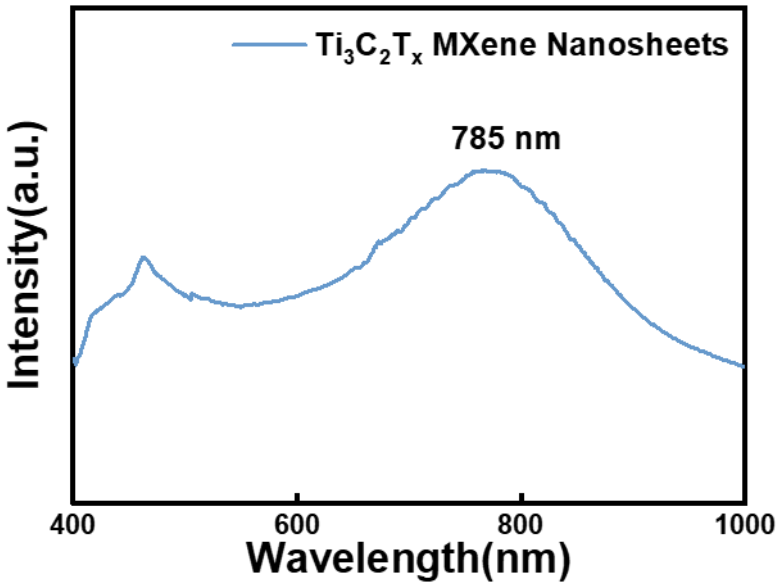

Figure S11. The UV–vis spectrum of $Ti_3C_2T_x$ MXene nanosheets.

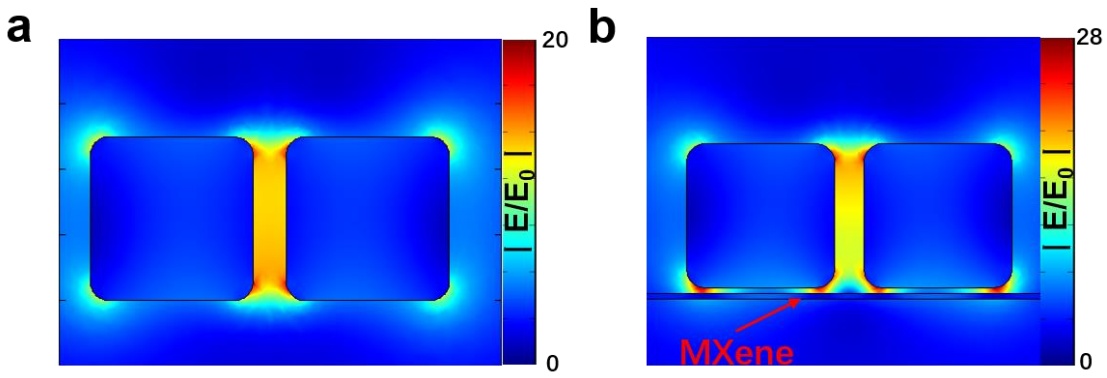

Figure S12. Electric field maps showing plasmonic coupling between adjacent AuNCs (a) without and (b) with a $Ti_3C_2T_x$ MXene nanosheet.

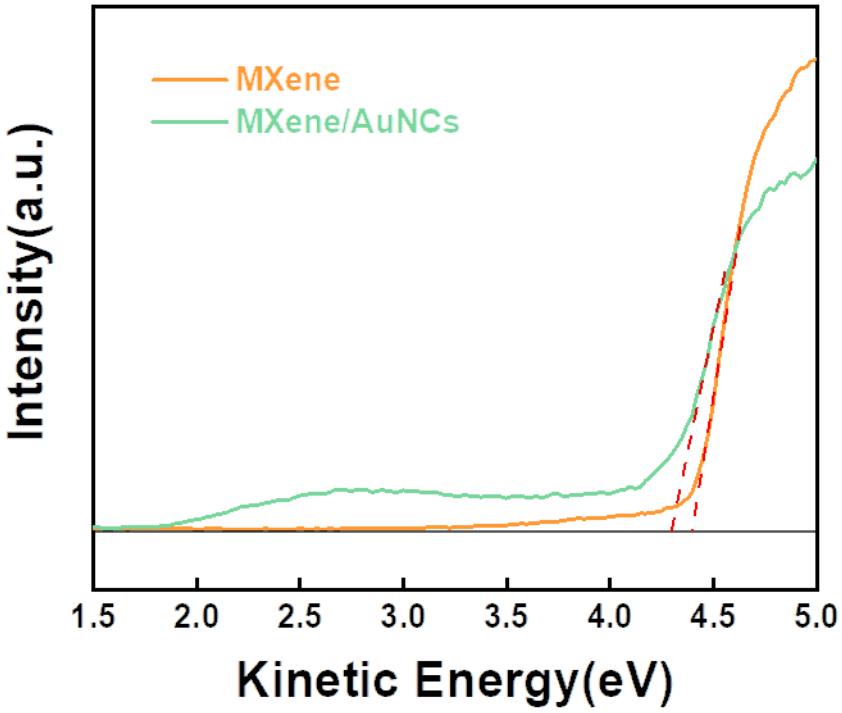

Figure S13. UPS of MXene and MXene/AuNCs membranes.

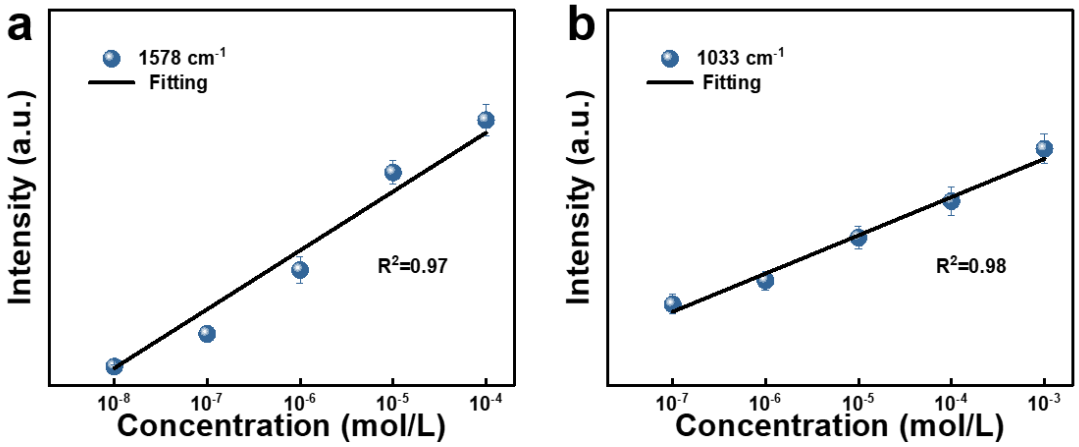

Figure S14. Linear fit between the characteristic peaks of (a) uric acid and (b) xanthine and the logarithm of the concentrations.

9. Supporting Tables

Table S1. The LOD and RSD of SERS substrates using R6G as the Raman reporter in previously reported and our work

Material	LOD	RSD	Ref.
MXene/Au NRs	10^{-12} M	18.1%	[5]
AgNPs/Leaf	1.2 μg/L	11.6%	[6]
MXene/Ag NPs	10^{-8} M	11.2%	[7]
GO/AgNPs	5×10^{-13} M	10.5%	[8]
MXene/AuNCs	10^{-13} M	51.94%	This Work
MXene/AuNCs-FOTS	10^{-14} M	6.41%	This Work

Table S2. Comparison of the SERS values and calculated value of the three mixtures

	612 cm^{-1}		**1618 cm^{-1}**	
	Experimental	Calculation	Experimental	Calculation
I	374. 73	379.37	1264. 47	1375.38
II	597. 26	587.70	138. 14	143.49
III	158. 89	155.07	82. 46	78.24

Table S3. The LOD of SERS substrates in previously reported and this work for uric acid.

Material	Sensitivity	with flexibility	Ref.
Au NRs/PDMS	10^{-6} M	Yes	[9]
Au NPs	1.1×10^{-4} M	No	[10]
Ag NPs	10^{-6} M	No	[11]
CdSe QDs	10^{-6} M	No	[12]
Ag-NPs@Cu-NW	5×10^{-8} M	No	[13]
Ti_3C_2-AuNCs	10^{-8} M	Yes	This work

Table S4. Comparison of SERS experimental values and calculated values of uric acid and xanthine.

	1578 cm^{-1}		**1033 cm^{-1}**	
	Experimental	Calculation	Experimental	Calculation
5×10^{-5} M	12921.8	12563.6	689.7	706.9
1×10^{-5} M	6355.5	6502.9	540.68	567.8
5×10^{-6} M	3606.1	3502.9	477.1	431.6
1×10^{-6} M	1592.4	1693.3	334.4	318.3
5×10^{-7} M	792.6	753.4	264.0	282.8

10. Determination of the limit of detection (LOD)

The LOD was determined based on serial dilutions of the solutions and performing SERS. In the case of R6G, for example, 612 cm^{-1} was selected as the characteristic peak, and SERS measurements were performed after serial dilution until the lowest concentration at which the characteristic peak could be clearly observed (signal-to-noise ratio greater than 3), and this concentration was determined as the LOD.

Reference:

[1] W. Haiss, N.T.K. Thanh, J. Aveyard, D.G. Fernig, Determination of Size and Concentration of Gold Nanoparticles from UV − Vis Spectra, Analytical Chemistry, 79(2007) 4215-21.https://doi.org/10.1021/ac0702084

[2] Y. Bai, K. Zhou, N. Srikanth, J.H.L. Pang, X. He, R. Wang, Dependence of elastic and optical properties on surface terminated groups in two-dimensional MXene monolayers: a first-principles study, RSC Advances, 6(2016) 35731-9.https://doi.org/10.1039/C6RA03090D

[3] G.R. Berdiyorov, Optical properties of functionalized Ti3C2T2 (T = F, O, OH) MXene: First-principles calculations, AIP Advances, 6(2016).https://doi.org/10.1063/1.4948799

[4] W. Niu, S. Zheng, D. Wang, X. Liu, H. Li, S. Han, et al., Selective Synthesis of Single-Crystalline Rhombic Dodecahedral, Octahedral, and Cubic Gold Nanocrystals, Journal of the American Chemical Society, 131(2009) 697-703.https://doi.org/10.1021/ja804115r

[5] H. Xie, P. Li, J. Shao, H. Huang, Y. Chen, Z. Jiang, et al., Electrostatic Self-Assembly of Ti3C2Tx MXene and Gold Nanorods as an Efficient Surface-Enhanced Raman Scattering Platform for Reliable and High-Sensitivity Determination of Organic Pollutants, ACS Sensors, 4(2019) 2303-10.https://doi.org/10.1021/acssensors.9b00778

[6] S.-Y. Chou, C.-C. Yu, Y.-T. Yen, K.-T. Lin, H.-L. Chen, W.-F. Su, Romantic Story or Raman Scattering? Rose Petals as Ecofriendly, Low-Cost Substrates for Ultrasensitive Surface-Enhanced Raman Scattering, Analytical Chemistry, 87(2015) 6017-24.https://doi.org/10.1021/acs.analchem.5b00551

[7] Y. Ye, W. Yi, W. Liu, Y. Zhou, H. Bai, J. Li, et al., Remarkable surface-enhanced Raman scattering of highly crystalline monolayer Ti3C2 nanosheets, Science China Materials, 63(2020) 794-805.https://doi.org/10.1007/s40843-020-1283-8

[8] Z. Cao, P. He, T. Huang, S. Yang, S. Han, X. Wang, et al., Plasmonic Coupling of AgNPs near Graphene Edges: A Cross-Section Strategy for High-Performance SERS Sensing, Chemistry of Materials, 32(2020) 3813-22.https://doi.org/10.1021/acs.chemmater.9b05293

[9] U. Mogera, H. Guo, M. Namkoong, M.S. Rahman, T. Nguyen, L. Tian, Wearable plasmonic paper–based microfluidics for continuous sweat analysis, Science Advances, 8 eabn1736.https://doi.org/10.1126/sciadv.abn1736

[10] J.E.L. Villa, R.J. Poppi, A portable SERS method for the determination of uric acid using a paper-based substrate and multivariate curve resolution, Analyst, 141(2016) 1966-72.https://doi.org/10.1039/C5AN02398J

[11] M. Pucetaite, M. Velicka, J. Pilipavicius, A. Beganskiene, J. Ceponkus, V. Sablinskas, Uric acid detection by means of SERS spectroscopy on dried Ag colloidal drops, Journal of Raman Spectroscopy, 47(2016) 681-6.https://doi.org/https://doi.org/10.1002/jrs.4875

[12] K. Wang, Z. Chen, Y. Li, Y. Zhang, Top-down produced CdSe quantum dots as an ultrasensitive SERS platform for the detection of uric acid, Materials Chemistry Frontiers, 7(2023) 1624-32.https://doi.org/10.1039/D2QM01275H

[13] Z. Song, S. Chen, Q. He, H. Liang, G. Huang, P. Li, et al., Floating Ag-NPs@Cu-NW bundles fabricated on copper mesh for highly sensitive SERS detection of uric acid in pretreatment-free urine, Analyst, 147(2022) 5670-9.https://doi.org/10.1039/D2AN01586B